

Journal Pre-proof

Phytoremediation of phenol by *Hydrilla verticillata* (L.f.) Royle and associated effects on physiological parameters

Guohua Chang, Bin Yue, Tianpeng Gao, Wende Yan, Gang Pan



PII: S0304-3894(19)31523-7

DOI: <https://doi.org/10.1016/j.jhazmat.2019.121569>

Reference: HAZMAT 121569

To appear in: *Journal of Hazardous Materials*

Received Date: 8 August 2019

Revised Date: 17 October 2019

Accepted Date: 29 October 2019

Please cite this article as: Chang G, Yue B, Gao T, Yan W, Pan G, Phytoremediation of phenol by *Hydrilla verticillata* (L.f.) Royle and associated effects on physiological parameters, *Journal of Hazardous Materials* (2019), doi: <https://doi.org/10.1016/j.jhazmat.2019.121569>

This is a PDF file of an article that has undergone enhancements after acceptance, such as the addition of a cover page and metadata, and formatting for readability, but it is not yet the definitive version of record. This version will undergo additional copyediting, typesetting and review before it is published in its final form, but we are providing this version to give early visibility of the article. Please note that, during the production process, errors may be discovered which could affect the content, and all legal disclaimers that apply to the journal pertain.

© 2019 Published by Elsevier.

Phytoremediation of phenol by *Hydrilla verticillata* (L.f.) Royle and associated effects on physiological parameters

Guohua Chang^a, Bin Yue^a, Tianpeng Gao^a, Wende Yan^{b*}, Gang Pan^{c,d*}

^a*School of Geography and Environmental Engineering, Lanzhou City University, The Engineering Research Center of Mining Pollution Treatment and Ecological Restoration of Gansu Province, Gansu 730070, China*

^b*Research Section of Ecology, Central South University of Forestry and Technology, Changsha 410004, Hunan, China*

^c*State Key Laboratory of Environmental Aquatic Chemistry, Research Center for Eco-Environmental Sciences, Chinese Academy of Sciences, Beijing 100085, China*

^d*School of Animal, Rural and Environmental Sciences, Nottingham Trent University, Nottingham 999020, UK*

Highlights

- *Hydrilla verticillata* can effectively remove phenol ($\leq 100 \text{ mg L}^{-1}$).
- Endogenous soluble organic compounds in *Hydrilla verticillata* were analyzed and identified.
- During phenol decomposition, unsaturated fatty acids content decreased significantly.

Abstract

Phenol contamination is a common occurrence in aquatic environments in different

parts of the world and strategies that utilize cheap and eco-friendly phytoremediation technologies are required to overcome associated environmental problems. In the present study, the submersed macrophyte *Hydrilla verticillata* (L.F.) Royle was exposed to different concentrations of phenol (0–200 mg L⁻¹) to assess its potential in phenol treatment. *H. verticillata* efficiently degraded phenol in solutions with initial concentrations lower than 200 mg L⁻¹. The adverse effects of phenol on physiological parameters of *H. verticillata* were also investigated after 7 d of phenol stress. In order to explore the effect of phenol on the metabolism of *H. verticillata* during phytoremediation, gas chromatography-mass spectrometry (GC-MS) was used to analyze endogenous soluble organic compounds. The results revealed the presence of greater than 60 soluble organic compounds in *H. verticillata*. In the process of phenol degradation, fatty acid composition and carbon number distribution were affected in the plants while unsaturated fatty acid content was significantly lower, and several compounds including aliphatic dicarboxylic acids and aromatic ketones were degraded while new compounds were synthesized by the plant. In summary, *H. verticillata* is a promising candidate for the phytoremediation of the phenol-contaminated aquatic system.

Keywords: Phenol; Phytoremediation; *Hydrilla verticillata*; Organic components

1. Introduction

Phenol is one of the most common organic water pollutants and is present in effluents released from multifarious processes including coal processing, phenol manufacture

and polymeric resin production [1]. The extensive use of phenol has led to widespread contamination of water and soil; this occurrence results in toxicity in living organisms due to the bioaccumulation of phenol [2, 3]. Phenol also contributes to off-flavors in drinking and food-processing waters. During the process of drinking water treatment, phenols can combine with chlorine to significantly contribute to chlorination disinfection by-products [4]. Phenol is also toxic to humans; overexposure can lead to coma, convulsions, cyanosis and death [1, 5]. Due to the toxicity and frequent occurrence of phenol in a wide range of aquatic environments, it is of great importance that efficacious, economical and eco-friendly technologies for the removal of phenol from contaminated water are investigated.

Several methods have been published for the removal of phenol; reported strategies have involved different reactions including chemical oxidation, electrochemical oxidation, microbial degradation, and phytoremediation [1, 3, 5]. In fact, when the concentration of phenol in wastes is small and the amount of polluted water is relatively large, abatement techniques that can be performed without the requirement for either other reactants (in particular bases or acids) or excessive amounts of energy should be preferentially used to better preserve the environment [1]. In recent years, phytoremediation, the use of green plants to extract, sequester and detoxify organic or inorganic pollutants [6, 7], has evoked much interest. These strategies encompass cheap, efficient, eco-friendly and solar-driven technologies with good public acceptance [7]. Several reports have been published pertaining to the use of plants such as vetiver root [8, 9], alfalfa [10], willow trees [11] and the hairy roots of

Helianthus annuus L. [5] for the remediation of phenol. Phenrat et al. (2017) reported that phenol degradation by vetiver in real aerated wastewater involves two phases: Phase I, phytopolymerization and phyto-oxidation assisted by root-produced peroxide (H_2O_2) and peroxidase (POD), followed by phase II, similar to phase I with enhanced rhizomicrobial degradation [9]. Teeratitayangkul et al. (2019) observed that maturation of plantlets results in an increase in the root biomass; this phenomenon results in both the release of increased levels of peroxidase and enhanced superoxide dismutase activity. The former occurrence accelerates phenol transformation, while the latter decreases the side effects associated with phenol detoxification [8].

In this study, we focused on *H. verticillata*, an aquatic plant found widely in freshwater habitats. This plant has not yet been investigated for its effectiveness in relation to phenol phytoremediation. *H. verticillata* is a rooted, submerged and perennial species that is widely distributed in most continents [12]. The plant grows quickly and has the potential to uptake and accumulate As and U [12, 13] as well as organic pesticides [14]. In this study, the ability of *H. verticillata* to remove phenol was explored and the responses of *H. verticillata* to phenolic stress were investigated. Concomitantly, to further investigate the effects of phenol on *H. verticillata* along with the absorption mechanisms that underpin phenol degradation, organic matter composition in the plant were analyzed in detail by GC–MS. These results provide us with new and important information that will help us to better understand phenol degradation while also revealing the mechanisms that underlie phenol degradation in the plant.

2. Materials and Methods

2.1. Phenol removal assays

H. verticillata was purchased from the local bird and flower market and cultured in 10% Hoagland's solution [15] prior to analysis. Phenol (> 99% purity) was used without further purification. Phenol concentrations (0, 20, 40, 60, 80, 100 and 200 mg L⁻¹) were used for subsequent experiments. Plants (35.0 ± 0.1 g, about 27 cm in length) with well-grown tips were exposed to varying concentrations of phenol (4 L) in colorless transparent containers (5 L). The containers were subsequently covered with a plastic wrap in order to prevent volatilization when exposed to a light intensity of 120 μmol m⁻² s⁻¹ and a 12-h photoperiod at 21/16°C; corresponding phenol solutions (containing 20, 40, 60, 80, 100 and 200 mg L⁻¹ phenol) served as controls. The phenol concentration was determined every 24 h [16]. After 7 d of cultivation, the plants were carefully washed with ultrapure water and blotted using filter paper. Finally, the fresh weight (FW) and organic matter composition of the plants were analyzed along with various other physiological parameters including protein, free amino acid (FAA), and soluble sugar levels in order to investigate the *Hydrilla verticillata*-mediated phenol degradation mechanisms; the effects of phenol on the plant were also assessed.

2.2. Analysis of photosynthetic pigments

Fresh plant samples (0.2 g) were homogenized with 95% (v/v) ethanol. The absorbance of each sample was measured at 665, 649 and 470 nm by spectrophotometry [17].

2.3. Dissolved protein and FAA analyses

Quantitative protein determination in fresh samples was achieved using coomassie bright blue G-250 at 595 nm with bovine serum albumin as the standard [18]. The amino acid content in the plant samples was measured by ninhydrin assays [19]. Each sample was measured spectrophotometrically at 570 nm and the results were expressed as mg g^{-1} FW.

2.4. Assay of soluble sugars

The amount of soluble sugar was determined using the anthrone-sulfuric acid method [18]. The sample was measured spectrophotometrically at 630 nm and the result was expressed as mg g^{-1} FW.

2.5. Determination of ascorbic acid (AsA)

The ascorbic acid was extracted from fresh plant material and titrated using 2,6-dichlorophenol-indophenol as previously described by Tu et al. [20]. The concentration of AsA was expressed as $\text{mg}/100$ g FW.

2.6. Determination of MDA

The MDA content in fresh samples was determined using thiobarbituric acid [21]. Fresh samples (1.0 g) were homogenized in 10% trichloroacetic acid (TCA) and centrifuged at 5,000 g for 10 min. Supernatant mixed with 0.6% thiobarbituric acid was measured spectrophotometrically at 450, 532 and 600 nm. MDA content was expressed as nmol g^{-1} FW.

2.7. Determination of superoxide anion

Superoxide anion radical ($\text{O}_2^{\cdot-}$) production was measured by monitoring nitrite

formation from hydroxylamine at 530 nm with NaNO_2 as the standard and the generation rate of $\text{O}_2^- \cdot$ was expressed as $\text{nmol min}^{-1} \text{g}^{-1} \text{FW}$ [22].

2.8. Determination of enzyme activities

Peroxidase (POD) activity in fresh samples was determined using 2-methoxyphenol (guaiacol) substrate in the presence of hydrogen peroxide and the activity was expressed as $\text{U min}^{-1} \text{g}^{-1} \text{FW}$ [22]. SOD activity was assayed by nitroblue tetrazolium (NBT) spectrophotometry at 560 nm [22].

2.9. High performance liquid chromatography (HPLC) analysis

HPLC analysis of samples was carried out using a modified version of a method published by Jha et al. [5]. Briefly, fresh tissue (0.5 g) was homogenized in 5 mL of methanol and centrifuged at 12,000 g for 10 min at 4°C. The supernatant filtered through a 0.22- μm membrane was analyzed by HPLC (SHIMADZU 10AVP) using a chromatographic column (SHIM-PACK VP-ODS- 150 \times 4.6 mm ID).

Chromatographic separation was achieved using a C18 column with methanol-water (70: 30) as the mobile phase, using a UV- absorbance detector (at 270 nm) and a 1.0 mL min^{-1} flow rate.

2.10. GC-MS Analysis

After 7 d, the samples (control and treated samples exposed to 200 mg L^{-1} of phenol) were removed from the phenol solution and cleaned several times in ultra-pure water, followed by naturally drying in shaded conditions.

GC-MS analysis was based on a modified version of a method published by Duan [23]. Briefly, samples of plant powder were sieved (< 80 mesh size), after being

ground at 4°C. Next, the samples (3.0 g) were extracted with CHCl₃: CH₃OH (3: 1, v/v) following 3 separate ultrasonic treatments (30 minutes each); the extracts were subsequently mixed. Lipids of plants were isolated and accurately weighed after natural volatilization of the extraction solvent. Asphaltene was subsequently generated from the extracted lipids by *n*-hexane precipitation and the residual soluble organic matter that remained was separated by column chromatography (alumina: silica gel, 1: 3). The saturated hydrocarbon (non-polar), aromatic hydrocarbon (weak polarity) and polar (non-hydrocarbon) fractions were eluted with *n*-hexane, dichloromethane and methanol, respectively. The composition of all fractions was analyzed by GC-MS (GC6890N/MSD5973N) equipped with a J&W HP-5 column (30 m × 0.32 mm i.d. × 0.25-μm film thickness). The oven temperature was raised from 80°C to 295°C with a heating rate of 4°C min⁻¹ and held stable for 30 min. The carrier gas was helium, and the column flow rate was 1.0 mL·min⁻¹. The MS conditions were as follows: electron ionization (EI) at 70 eV; an ion source temperature of 230°C; quadrupole rod temperature of 150°C, interface temperature of 280°C and spectrum library with NIST05L (U.S.A.). The separation process is shown in Fig. S1 of the supporting materials.

2.11. Statistical analysis

The experimental data were assessed using one-way analysis of variance (ANOVA) and statistical significance was set at the level of $P < 0.05$.

3. Results

3.1. Effects of *H. verticillata* on phenol concentration

Compared with the control, a continuous reduction in the concentration of phenol was observed following co-incubation with plants (Fig. 1). When the level of phenol was 20 mg L^{-1} , the phenol concentration decreased by 78% after 3 d of treatment, and the phenol content was reduced to almost the level of the control after 5 d. Similar decreasing trends were also observed at other treatment levels (from 40 to 100 mg/L). Upon application of the highest level (200 mg L^{-1}) of phenol, the reduction rate was lower than that observed for lower levels ($\leq 100 \text{ mg L}^{-1}$) during the incubation period. Phenol is very soluble in water and has a low vapor pressure. According to the control experiments for each level of phenol solution (without plants), the natural loss of phenol was very low during the incubation period and phenol volatilization was not the main reason for its disappearance from the solution under the assay conditions, which was also confirmed by the findings of Flocco et al. [10]. Hence, *H. verticillata* played an important role in removing phenol from solution.

(FIGURE 1)

The relationship between phenol concentration and incubation time in the presence of *Hydrilla verticillata* can initially be described by the following non-linear regression equation (dot lines in Fig. 1):

$$C = \frac{C_0}{1 + \exp\left(A - \frac{B}{t+1}\right)}$$

where C is the amount of phenol in solution at t moment, C_0 is the initial amount of phenol in solution, A and B are the regression constants, and t is the time elapsed. The kinetic parameters and square of the correlation coefficient (R^2) are shown in Table 1.

The mean value of $t_{1/2}$ (the half-life of phenol) in the presence of the *Hydrilla*

verticillata system was calculated when C was $1/2C_0$; the results are shown in Table 1.

The half-life of phenol in the presence of the *Hydrilla verticillata* system gradually increased following phenolic stress. When *Hydrilla verticillata* was exposed to the highest concentration of phenol (200 mg L^{-1}), acute effects such as yellowing of leaves were observed and the theoretical half-life of phenol was calculated for this concentration.

(Table 1)

3.2. Physiological parameter analysis

The chl-*a* content in plants decreased gradually with increasing phenol concentrations (Table 2). No significant differences were observed for chl-*b* and car in plants following phenolic stress. The total chlorophylls-to-carotenoids ratio also significantly decreased in plants following exposure to the highest level of phenol (200 mg L^{-1}) compared with the control.

(Table 2)

The effects of phenol on proteins, FAA, soluble sugars, AsA, SOD, and O_2^- in plants are shown in Table 2. A negative correlation existed between phenol concentration and protein content in plants. When the level of phenol was 60 mg L^{-1} , there was a significant reduction in protein content compared with the control. Similar to protein, the FAA content and FW decreased with increasing phenol concentrations. However, treatment with 200 mg L^{-1} phenol caused a 2.68-fold increase in soluble sugar content in plants, compared with the control samples. The AsA content of plants increased gradually until stabilizing at a concentration of 80 mg L^{-1} . Within the range

of 0–200 mg L⁻¹ phenol, there was a maximum increase of 160% in MDA content (61.0 nmol g⁻¹ FW at 60 mg L⁻¹ phenol) compared with the control.

POD activity in plants remained stable at < 80 mg L⁻¹ phenol, and then increased gradually. SOD activity initially increased with increasing phenol concentration and then gradually decreased. The change in the rate of O₂^{-·} production was similar to the profile observed for SOD activity. The maximum increase in O₂^{-·} level was 122% in the plant exposed to phenol at 60 mg L⁻¹.

The correlation analysis of physiological and biochemical parameters of the plant are presented in Table 3. Phenol concentration was negatively correlated with chl-*a* and *b* in *Hydrilla verticillata* (-0.941 and -0.951, at the level of $p = 0.01$); the phenol concentration was also negatively correlated with carotene, protein, FAA and POD enzyme levels. However, a positive correlation was observed between phenol concentration and AsA and soluble sugars. Chlorophyll *a* was positively correlated with chl-*b*, protein and FAA, with correlation coefficients of 0.890, 0.899 and 0.797, respectively. There was a significant positive correlation between protein and FAA content following exposure to phenol (0.938, $p = 0.01$); however, protein was negatively correlated with AsA content (-0.995, $p = 0.01$), and FAA content in plants was also negatively correlated with AsA content (-0.995, $p = 0.01$). There was a very significant negative correlation between the changes in soluble sugar and AsA content (-0.947, $p = 0.01$). Alterations in the AsA content were positively correlated with changes in SOD enzyme levels (0.876, $p = 0.01$). The change in the MDA content was positively correlated with the changes to SOD enzyme and O₂^{-·} levels (0.781 and

0.780, $p = 0.05$). These results demonstrate that the absorption and degradation of phenol in *Hydrilla verticillata* have considerable effects on photosynthesis, protein metabolism and antioxidant systems in the analyzed plants.

(Table 3)

3.3. HPLC analysis

A common peak eluting at 1.9 min was observed in the HPLC chromatograms of untreated plants and plants treated with 100 and 200 mg L⁻¹ phenol (Figs. 2A, B and C). The peak eluting at 2.9 min corresponding to pure phenol (in Fig. 2D) was not observed in the chromatograms of plants; the same results were observed in plants treated with lower concentrations of phenol (data not shown). These results demonstrate that phenol can be transformed by *H. verticillata*.

(FIGURE 2)

3.4. GC-MS analysis

3.4.1. Non-polar fraction analysis

A total of 19 non-polar components were observed in *H. verticillata* samples; these components were predominantly composed of *n*-alkanes and isoprenoid alkanes (norpristane, pristane and phytane) (Fig. S2 and Table 4). The carbon number distribution range of the *n*-alkanes was C₁₅-C₂₉; tricosane represented the main peak in *H. verticillata*. In general, the percentage of alkanes with an odd number of carbons was higher than the percentage of alkanes with an even number of carbons. The relative abundance of the top three *n*-alkanes was as follows: C₂₃ (31.858%) > C₂₁ (22.988%) > C₂₅ (11.403%), respectively.

Compared with the control, phenol had no effect on the composition of the non-polar fraction in plants but affected the relative abundance of heneicosan and heptacosane in the treated samples significantly (Table 4).

(Table 4)

Alkanes, which play important roles in moderating gas exchange, protecting plants against ultraviolet radiation and extreme temperature damage and providing mechanical support to maintain the integrity of plant organs, are the main chemical constituents in plant wax [24]. *H. verticillata* is a single leaf perennial submerged plant with *n*-C₂₃ representing the main *n*-alkane peak; its total carbon advantage index (CPI_{total-1}) value is 4.58 (Table 5). In general, most plants have a higher prevalence of odd carbon than even carbon alkanes, with CPI values between 4.0 and 29.7.

Terrestrial higher plants predominantly contain *n*-alkanes with 25–31 carbons and high CPI values. *n*-C₂₃ or *n*-C₂₅ alkanes are the dominant compounds in aquatic submerged plants [25]. The prevalence of *n*-alkanes in *H. verticillata* is consistent with the afore-mentioned characteristics of aquatic submerged plants. Phenolic stress did not result in a significant difference in the CPI_{total} of *H. verticillata*; however, it had a clear effect on OEP and the $\sum C_{21}^- / \sum C_{22}^+$ ratio, which indicates that higher carbon number *n*-alkanes may have been selectively degraded in the plant (Table 5).

(Table 5)

In addition, a small amount of PMI was detected in plants. This compound is generally considered to be a sedimentary biological marker for methanogenic bacteria [26]. Although the presence of this substance in *H. verticillata* might help to reveal

the composition of associated sediments, the relationship between the plant and methanogenic bacteria remains to be elucidated.

3.4.2. Weak polarity fraction analysis

In total, 16 weakly polar components, namely neophytadienes, alkylfurans and polycyclic aromatic hydrocarbons, were observed for the control samples (Fig. S3 and Table 6). The main peak that was observed contained neophytadiene with a relative abundance of 60.759% compared with the other components. Although phenol stress had no effect on the species of weak polar fraction in *H. verticillata*, there was significant variation in relation to the abundance of the weak polarity fraction, especially for the main component, neophytadiene (Table 6). The abundance of neophytadiene in the treated samples was 48.26%, a reduction of 20.6% compared with the control. Neophytadiene was derived from the chlorophyll-side chain—the dehydrated derivative of phytanol, and the precursor of the isoprenoid alkenes in the non-polar fractions (norpristane, pristane, and phytane) [27]. Under phenol stress, the content of chl-*a* decreased gradually with concomitant increases in the phenol concentration; this phenomenon might be related to the simultaneous reduction of neophytadiene. Polycyclic aromatic hydrocarbons (Phenanthrene, fluoranthene and pyrene) were detected both in the control and treated samples. This result suggests that the aforementioned substances may have been absorbed by plants from the surrounding environment.

(Table 6)

3.4.3. Polar fraction analysis

The polar fraction components detected in the control samples consisted mainly of C₁₂-C₂₄ fatty acid compounds, with a relative abundance of 83.7% (Fig. 3 and Table 7). The other components consisted of aromatic acids and aromatic ketone, with abundances of less than 5%. Among the fatty acids that were observed, the *n*-hexadecanoic acid content was the highest (37.34%), and the abundances of the other fatty acids were all below 15%. In biological systems, fatty acids usually contain an even number of carbon atoms, typically between 12 and 24 [28]. The main components of the observed unsaturated fatty acids in *H. verticillata* were α -linolenic acid and linoleic acid.

(FIGURE 3)

(Table 7)

In treated samples, there were 22 different kinds of polar fraction compounds which were divided into three types: fatty acids, carboxylic acid compounds containing carbonyl groups and carboxylic acid compounds containing furan groups. The main components detected in the polar fraction in the treated samples were C₁₄-C₂₆ fatty acids, with a relative abundance of up to 95.2% (Fig. 4 and Table 8). Among the various fatty acids, *n*-hexadecanoic acid was the most prevalent (47.06%), and the total amount of saturated fatty acids was almost three times greater than the total amount of unsaturated fatty acids. Among the saturated fatty acid compounds, the abundance of even carbon compounds was greater than that of adjacent odd carbon compounds.

(FIGURE 4)

(Table 8)

Compared with the control sample, a total of 7 compounds containing a benzene ring were not detected in the treated samples. Furanone ($C_{11}H_{16}O_2$) and the compounds containing aliphatic dicarboxylic acids observed in the control were not detected in the treated sample, and three new compounds (10-oxo-decanoic acid, methyl 10-oxo-8-decenoate and methyl-8-(2-furyl) octanoate) were contained in the treated samples. Thus, during phenol conversion, compounds including aromatic acid, furan ketones and aromatic ketones with a benzene ring and/or carbonyl and carboxyl side-chains were selectively degraded in the plant. Among this new generation of compounds, methyl, 8-(2-furyl) octanoate was the only compound containing furan functional groups in the treated samples, which may be derived from tetrahydro-4,4,7-trimethyl-2 (4H) -benzofuranone. The carbonyl group of the benzofuran ring can be reduced to a hydroxyl group by hydrogenation. Carbon-carbon double bonds in the furan ring are subsequently formed by dehydration of the hydroxyl and adjacent hydrogen atoms. It is possible that the carbon bond that connects the two methyl groups in the benzene ring and the common carbon of the benzofuran ring might break with an opening in the aromatic ring occurring; the methyl group in the aromatic ring might subsequently be oxidized to carboxylic acid, with the methyl group being removed and the concomitant generation of the final product methyl, 8-(2-furyl) octanoate. Compared with the control, the carbon number distribution, $CPI_{total-2}$ and the rate of \sum unsaturated fatty acids and \sum saturated fatty acids of the treated samples were altered (Table 5).

3.4.4. Chromatographic column composition

The lipid composition of plants was analyzed by column chromatographic family composition analysis (Table S1). In the control sample, asphaltene, which is mainly present in proteins and polysaccharides, had the highest relative abundance of 69.13%, and the relative abundances of other fractions were as follows: polar fractions > weak polarity fractions > non-polar fractions. When phenol was absorbed and converted by plants, polar fractions and weak polarity fractions were decreased.

4. Discussion

In the present study, the phenol content in the presence of plants significantly decreased with increasing incubation times. Chl-*a* is an essential pigment for oxygenic photosynthesis; this pigment is important in all oxygenic photosynthetic organisms [29]. The decrease in chl-*a* content following phenolic stress directly affected photosynthesis in plants. The maximum reduction in chl-*a* content at the highest phenol concentrations (200 mg L⁻¹) may be due to the disruption of chloroplasts or changes in the lipid-to-protein ratio in pigment-protein complexes. The latter phenomenon may also have been caused by increased chlorophyllase activity [30]. The decrease in chl-*a* content was correlated with the macroscopic phenomenon of yellowing of some leaves. In addition, *H. verticillata* gradually grew some new roots in phenol solutions with concentrations less than 100 mg L⁻¹. No new roots were observed in the presence of 200 mg L⁻¹ phenol following 7 d of treatment. The synthesis of chl-*b* involves oxygenation of the 7-methyl group of chl-*a* to a formyl group in the presence of molecular oxygen, a reaction that is catalyzed by the enzyme chlorophyllide and oxygenase [31]. Following analysis of the effect of phenolic stress

on pigment content, we observed that chl-*a* was inhibited; however, the subsequent conversion of chl-*a* to chl-*b* was not affected. Carotenoids, as non-enzymatic antioxidants, can protect chlorophyll pigments under metal stress, and an increased or constant level of total carotenoids can act as a defense strategy for plants [32, 17]. Similarly, our studies reveal that the level of carotenoids in plants remains stable under phenolic stress (Table 2). Large amounts of chlorophyll are synthesized during plant growth and broken-down during senescence, and in green leaves, chlorophyll is subject to constant turnover [33]. During biotic or abiotic stress or during leaf senescence, metabolism shifts from anabolism to catabolism, and there is a significant increase in chlorophyll degradation [33]. Hence, it can be concluded that phenol removal in plants treated with 200 mg L⁻¹ phenol can result in a switch in chl-*a* metabolism from anabolism to catabolism.

The protein content was gradually reduced with increasing concentrations of phenol (Table 2). This latter phenomenon caused a change in the fresh weight of plants. The associated decrease may have resulted from adverse effects of phenol metabolism on protein synthesis or proteolysis. Amino acids have a variety of important functions or roles in plants including protein biosynthesis, encoding building blocks for several other biosynthesis pathways and playing pivotal roles during signaling processes as well as during plant stress responses [34]. The reduction of FAA in plants is likely to be directly related to the reduction in protein levels following phenolic stress.

Degradation of photosynthesis-associated proteins is an important aspect of nutrient mobilization during stress [33]. This phenomenon suggests that chl-*a* likely plays an

important role in protein biosynthesis in plants, which is also confirmed by the correlation analysis of physiological parameters of *H. verticillata* (Table 3).

Increases in soluble sugar levels following exposure to increasing phenol concentrations may be related to increased osmotic pressures associated with phenol solutions (Table 2). The increased osmotic pressure of phenol solutions at higher concentrations could inhibit and retard the germination of seeds from common crops (*P. mungo* and *T. aestivum*) [5].

AsA is a widespread metabolite synthesized by plant cells. This metabolite is involved in numerous processes among which antioxidative activity is the most prominent [35]. The increased levels of O_2^- observed suggest that the absorption and conversion of phenol by the plant stimulates free radical-generating capacity. In the present study, the accumulation of AsA in plants in response to stresses is likely required to facilitate scavenging of reactive oxygen species.

MDA is a cytotoxic product of membrane lipid peroxidation and MDA levels are considered a measure of lipid peroxidation status. Lipid peroxidation is linked to the production of O_2^- [36]. MDA and O_2^- levels had similar profiles in plants following phenol stress, and a positive correlation was observed between these parameters (Table 3).

Antioxidant enzymes in plants play an important role in their adaptation and tolerance to environmental stresses. In fact, the activities of antioxidative enzymes are inducible by oxidative stress [37]. This phenomenon most likely reflects a general strategy required to overcome stress [38]. A significant increase in the activity of

POD was observed when *H. verticillata* was exposed to 200 mg L⁻¹ of phenol (Table 2). Singh et al. also reported that phenol removal was associated with the inherent production of peroxidase and hydrogen peroxide in *V. zizanioides* plantlets [6]. Similar results were reported by Jha et al. [5] and Flocco et al. [10]. The latter studies suggested that plant peroxidase is associated with the transformation and detoxification of phenol. Increased peroxidase levels are also thought to protect plant cells from free radical oxidation, allowing plants to adapt to associated stressors [10, 39]. SOD as an essential component of the plant antioxidative defense system, dismutates two O₂⁻· to water and oxygen [40]. The generation of ROS such as O₂⁻· and H₂O₂ is a common event associated with normal plant biochemical processes. The latter radicals are also likely to be generated when plants are exposed to stresses [6]. When the levels of ROS that are generated exceed the ability of the antioxidant system to cope with the associated stress, damage to cellular components inevitably occurs [36]. The resultant ROS can rapidly attack all types of biomolecules such as nucleic acids, proteins, lipids and amino acids, leading to irreparable metabolic dysfunction, membrane destruction, protein inactivation, DNA mutation and cell death [36, 41]. The present study reveals that metabolism of phenol could enhance the antioxidant enzyme activities of plants. At higher phenol concentrations, the formation of ROS may exceed the antioxidant scavenging capacity, which may lead to the damage of cellular components.

The results of HPLC analysis suggest that phenol is transformed by *H. verticillata*. The GC-MS analysis revealed that the non-polar fraction was predominantly

composed of *n*-alkanes, with relatively stable structures; the influence of phenol degradation on the non-polar fraction of the plant was minimal (Table 4, 5 and S1). During the absorption and conversion of phenol, the level of neophytadiene in the weak polarity fraction significantly decreased in plants following exposure to the highest level of phenol (200 mg L⁻¹) compared with the control (Table 6). The normal metabolism of fatty acid compounds in the body of the plant was greatly affected (Table 5, 7 - 8). The decomposition of fatty acid compounds was stimulated, leading to a significant decrease in the relative abundance of these compounds. Fatty acid composition and carbon number distribution were both affected; unsaturated fatty acid content was significantly lower and there was an increase in the synthesis of new long-chain saturated fatty acids. Azelaic acid is involved in plant systemic immunity and the priming of the host defense [42]. Compared with the controls, azelaic acid was not detected in the treated samples (Table 7 and 8), indicating that the absorption and degradation of phenol might impact systemic immunity in *H. verticillata*. In addition, the asphaltene content in the treated samples was greater than that observed for the control samples (Table S1). During the absorption and degradation of phenol, the protein content gradually decreased while the soluble sugar content increased with increasing phenol concentrations in *H. verticillata*, and therefore, the reduction in the fatty acid content in the plant may be closely related to its conversion to sugars and asphaltene in *H. verticillata*. Overall, the metabolism of phenol at higher concentrations significantly affected photosynthesis, protein metabolism, sugar metabolism and fatty acid metabolism in *Hydrilla verticillata*.

Recent research pertaining to phenol degradation by vetiver plantlets has revealed that hydrogen peroxide and POD produced by plant roots along with constituents of the rhizosphere microbiome all play an important role in phenol degradation in water [8, 9]. Hence, the degradation of phenol in water involves many factors including metabolic activities in plants, the release of substances from plants into water, and the activity of microorganisms; all of these factors affect the phytoremediation of phenol in water.

5. Conclusions

H. verticillata can effectively absorb and degrade phenol ($\leq 100 \text{ mg L}^{-1}$) without dramatically affecting associated physiological parameters, and the resultant degradation products are non-toxic. However, during phenol decomposition, neophytadiene content decreased significantly. At the same time, the unsaturated fatty acids in the plant body were more rapidly degraded following exposure to phenol. This study also reveals that plants have the potential to degrade exogenous pollutants containing hydrocarbons. Further studies are required to investigate plant restoration technologies for the degradation and elimination of organic pollutants in soil, water and even the atmosphere. In view of inherent fast growth rates, high biomass and wide distribution, *Hydrilla* plants appear to have great potential for the remediation of phenol pollution in aquatic environments.

Declaration of interests

The authors declare that they have no known competing financial interests or personal relationships

that could have appeared to influence the work reported in this paper.

The authors declare the following financial interests/personal relationships which may be considered as potential competing interests:

Acknowledgments

This research was funded by the National Natural Science Foundation of China (Grant No. 31860176) and the National Science & Technology Pillar Program of the 13th Five-year Plan (BAD07B05, 2015). We would like to thank LetPub (www.letpub.com) for providing linguistic assistance.

References

- [1] G. Busca, S. Berardinelli, C. Resini, L. Arrighi, Technologies for the removal of phenol from fluid streams: a short review of recent developments, *J. Hazard. Mater.* 160 (2008) 265–288.
- [2] L. Vittozzi, G.D. Angelis, A critical review of comparative acute toxicity data on freshwater fish, *Aquat. Toxicol.* 19 (1991) 167–204.
- [3] N.V. Pradeep, S. Anupama, K. Navya, H.N. Shalini, M. Idris, U.S. Hampannavar, Biological removal of phenol from wastewaters: a mini review, *Appl. Water Sci.* 5 (2015) 105–112.
- [4] F. Gea, L.Z. Zhua, H.R. Chen. Effects of pH on the chlorination process of phenols in drinking water, *J. Hazard. Mater.* 133 (2006) 99–105.
- [5] P. Jha, R. Jobby, S. Kudale, N. Modi, A. Dhaneshwar, N. Desai, Biodegradation of phenol using hairy roots of *Helianthus annuus* L, *Int. Biodeterior. Biodegrad.* 77 (2013) 106–113.
- [6] S. Singh, J.S. Melo, S. Eapen, S.F. D'Souza, Potential of vetiver (*Vetiveria zizanoides* L. Nash) for phytoremediation of phenol, *Ecotoxicol. Environ. Saf.* 71 (2008) 671–676.
- [7] H. Ali, E. Khan, M.A. Sajad, Phytoremediation of heavy metals—concepts and applications, *Chemosphere* 91 (2013) 869–881.
- [8] P. Teeratitayankul, C. Phutthasimma, S. Wichai, T. Phenrat, Rhizomicrobial-augmented mature vetiver root system rapidly degrades phenol in illegally dumped industrial wastewater, *Desalin. Water Treat.* 159 (2019) 40–52.
- [9] T. Phenrat, P. Teeratitayankul, I. Prasertsung, R. Parichatprecha, P. Jitsangiam, N. Chomchalow, S. Wichai, Vetiver plantlets in aerated system degrade phenol in illegally dumped industrial wastewater by phytochemical and rhizomicrobial degradation, *Environ. Sci. Pollut. Res.* 24 (2017) 13235–13246.
- [10] C.G. Flocco, A. Lobalbo, M.P. Carranza, A.M. Giuliotti, Removal of phenol by alfalfa plants

- (*Medicago sativa* L.) grown in hydroponics and its effect on some physiological parameters, *Acta Biotechnol.* 22 (2002) 43–54.
- [11] A.S. Ucisik, S. Trapp, Uptake, removal, accumulation, and phytotoxicity of phenol in willow trees (*Salix viminalis*), *Environ. Toxicol. Chem.* 25 (2006) 2455–2460.
- [12] S. Srivastava, S. Mishra, R.D. Tripathi, S. Dwivedi, P.K. Trivedi, P.K. Tandon, Phytochelatin and antioxidant systems respond differentially during arsenite and arsenate stress in *Hydrilla verticillata* (L.F.) Royle, *Environ. Sci. Technol.* 41 (2007) 2930–2936.
- [13] S. Srivastava, K.C. Bhainsa, S.F. D'Souza, Investigation of uranium accumulation potential and biochemical responses of an aquatic weed *Hydrilla verticillata* (L.f.) Royle, *Bioresour. Technol.* 101 (2010) 2573–2579.
- [14] M.L. Hinmant, S.J. Klaine, Uptake and translocation of selected organic pesticides by the rooted aquatic plant *Hydrilla verticillata* royle, *Environ. Sci. Technol.* 26 (1992) 609–613.
- [15] D.R. Hoagland, D.I. Arnon, The water-culture method for growing plants without soil, *Calif. Agric. Exp. Station Circ.* 347 (1950) 1–32.
- [16] R.W. Martin, Rapid colorimetric estimation of phenol, *Anal. Chem.* 21 (1949) 1419–1420.
- [17] M. Molnárová, A. Fargašová, Se(IV) phytotoxicity for monocotyledonae cereals (*Hordeum vulgare* L., *Triticum aestivum* L.) and dicotyledonae crops (*Sinapis alba* L., *Brassica napus* L.), *J. Hazard. Mater.* 172 (2009) 854–861.
- [18] G.H. Chang, Q. Zhang, L. Zhang, Y.J. Lü, T.P. Gao. Effects of sodium dodecyl sulfate on wheat (*Triticum Aestivum* L.) seedlings. *Environ. Prog. Sustain. Energy* 34 (2015) 1142–1147.
- [19] K.M. Saad-Allah, M.A. Elhaak. Hyperaccumulation activity and metabolic responses of

- Solanum nigrum* in two differentially polluted growth habitats, *J. Saudi Soc. Agric. Sci.* 16 (2015) 227–235.
- [20] J. Tu, M. Zhang, B.G. Xu, H.H. Liu. Effects of different freezing methods on the quality and microstructure of lotus (*Nelumbo nucifera*) root, *Int. J. Refrig.* 52 (2015) 59–65.
- [21] K. Tange, J.C. Zhan, H.R. Yang, W.D. Huang, Changes of resveratrol and antioxidant enzymes during UV-induced plant defense response in peanut seedlings, *J. Plant Physiol.* 167 (2010) 95–102.
- [22] G.L. Wu, J. Cui, L. Tao, H. Yang, Fluroxypyr triggers oxidative damage by producing superoxide and hydrogen peroxide in rice (*Oryza sativa*), *Ecotoxicology* 19 (2010) 124–132.
- [23] Y. Duan, Y.Z. Wu, X.X. Cao, Y. Zhao, L.H. Ma, Hydrogen isotope ratios of individual *n*-alkanes in plants from Gannan Gahai Lake (China) and surrounding area, *Org. Geochem.* 77 (2014) 96–105.
- [24] X. Wu, H. Yin, Z.B. Shi, Y.Y. Chen, K.J. Qi, X. Qiao, G.M. Wang, P. Cao, S.L. Zhang, Chemical composition and crystal morphology of epicuticular wax in mature fruits of 35 pear (*Pyrus* spp.) cultivars, *Front. Plant Sci.* 9 (2018) 679–693.
- [25] Y. Duan, L. Xu. Distributions of *n*-alkanes and their hydrogen isotopic composition in plants from Lake Qinghai (China) and the surrounding area, *Appl. Geochem.* 27 (2012) 806–814.
- [26] A.J. Vella, G. Holzer, Distribution of isoprenoid hydrocarbons and alkylbenzenes in immature sediments: evidence for direct inheritance from bacterial/algal sources, *Org. Geochem.* 18 (1992) 203–210.
- [27] J.F. Rontani, J.K. Volkman, Phytol degradation products as biogeochemical tracers in aquatic environments, *Org. Geochem.* 34 (2003) 1–35.

- [28] S. Petrovic, A. Arsic, Fatty acids: fatty acids, in: B. Caballero, P. M. Finglas, F. Toldrá (Eds.), Encyclopedia of food and health, Oxford, UK: Academic Press, 2016, pp. 623–631, DOI:10.1016/B978-0-12-384947-2.00277-4.
- [29] H. Miyashita, K. Adachi, N. Kurano, H. Ikemot, M. Chihara, S. Miyach, Pigment composition of a novel oxygenic photosynthetic prokaryote containing chlorophyll *d* as the major chlorophyll, *Plant Cell Physiol.* 38 (1997) 274–281.
- [30] A. Parida, A.B. Das, P. Das, NaCl stress causes changes in photosynthetic pigments, proteins, and other metabolic components in the leaves of a true mangrove, *Bruguiera parviflora*, in hydroponic cultures, *J. Plant Biol.* 45 (2002) 28–36.
- [31] L.L. Eggink, R. LoBrutto, D.C. Brune, J. Brusslan, A. Yamasoto, A. Tanaka, J.K. Hooper, Synthesis of chlorophyll *b*: localization of chlorophyllide *a* oxygenase and discovery of a stable radical in the catalytic subunit, *BMC Plant Biol.* 4 (2004) 5–20.
- [32] S. Singh, S. Sinha, R. Saxena, K. Pandey, K. Bhatt, Translocation of metals and its effects in the tomato plants grown on various amendments of tannery waste: evidence for involvement of antioxidants, *Chemosphere* 57 (2004) 91–99.
- [33] K. Gutbrod, J. Romer, P. Dörmann, Phytol metabolism in plants, *Prog. Lipid Res.* 74 (2019) 1–17.
- [34] T.M. Hildebrandt, A.N. Nesi., W.L. Araújo, H.P. Braun, Amino acid catabolism in plants, *Mol. Plant* 8 (2015) 1563–1579.
- [35] J. Kováèik , G. Rotková, M. Bujdoš , P. Babula , V. Peterková , P. Matúš, Ascorbic acid protects *Coccomyxa subellipsoidea* against metal toxicity through modulation of ROS/NO balance and metal uptake, *J. Hazard. Mater.* 339 (2017) 200–207.

- [36] M. Choudhary, U.K. Jetley, M.A. Khan, S. Zutshi, T. Fatma, Effect of heavy metal stress on proline, malondialdehyde, and superoxide dismutase activity in the cyanobacterium *Spirulina platensis*-S5, *Ecotoxicol. Environ. Saf.* 66 (2007) 204–209.
- [37] C.H. Foyer, P. Descourvières, K.J. Kunert, Protection against oxygen radicals: an important defense mechanism studied in transgenic plants, *Plant Cell Environ.* 17 (1994) 507–523.
- [38] N. Dinakar, P.C. Nagajyothi, S. Suresh, Y. Udaykiran, T. Damodharam, Phytotoxicity of cadmium on protein, proline and antioxidant enzyme activities in growing *Arachis hypogaea* L. seedlings, *J. Environ. Sci.* 20 (2008) 199–206.
- [39] J.S. Lytle, T.F. Lytle, Use of plants for toxicity assessment of estuarine ecosystems, *Environ. Toxicol. Chem.* 20 (2001) 68–83.
- [40] I. Cakmak, W.J. Horst, Effect of aluminium on lipid peroxidation, superoxide dismutase, catalase and peroxidase activities in root tips of soybean (*Glycine max*), *Physiol. Plant.* 83 (1991) 463–468.
- [41] C.M. Luna, C.A. González, V.S. Trippi, Oxidative damage caused by an excess of copper in oat leaves, *Plant Cell Physiol.* 35 (1994) 11–15.
- [42] H.W. Jung, T.J Tschaplinski, L. Wang, J. Glazebrook, J. T. Greenberg, Priming in systemic plant immunity, *Science* 324 (2009) 89–91.

Figure captions:

FIGURE 1. Change in phenol concentration versus time in the presence of *H. verticillata* and dot lines are non-linear regression curves (95% confidence).

FIGURE 1

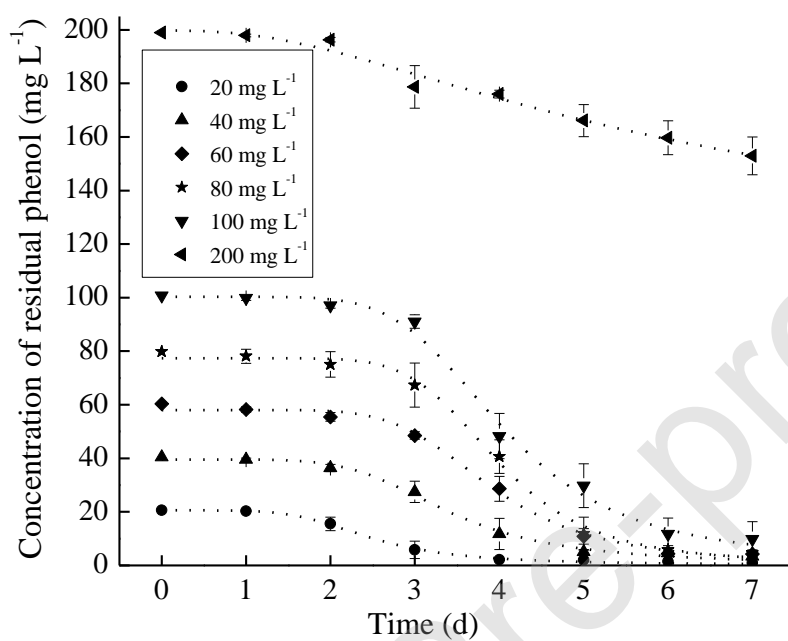


FIGURE 2. HPLC chromatograms of samples (A, *H. verticillata* treated with 200 mg L⁻¹ phenol; B, *H. verticillata* treated with 100 mg L⁻¹ phenol; C, Untreated *H. verticillata*; D, phenol).

FIGURE 2

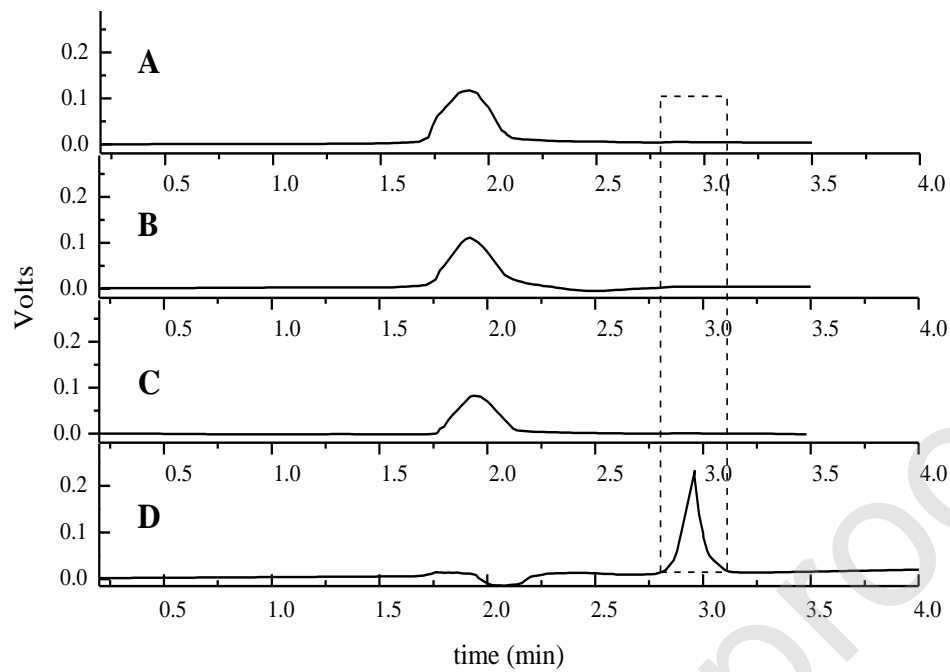


FIGURE 3. Total ion current chromatogram of polar fraction in control sample from *H. verticillata*.

FIGURE 3

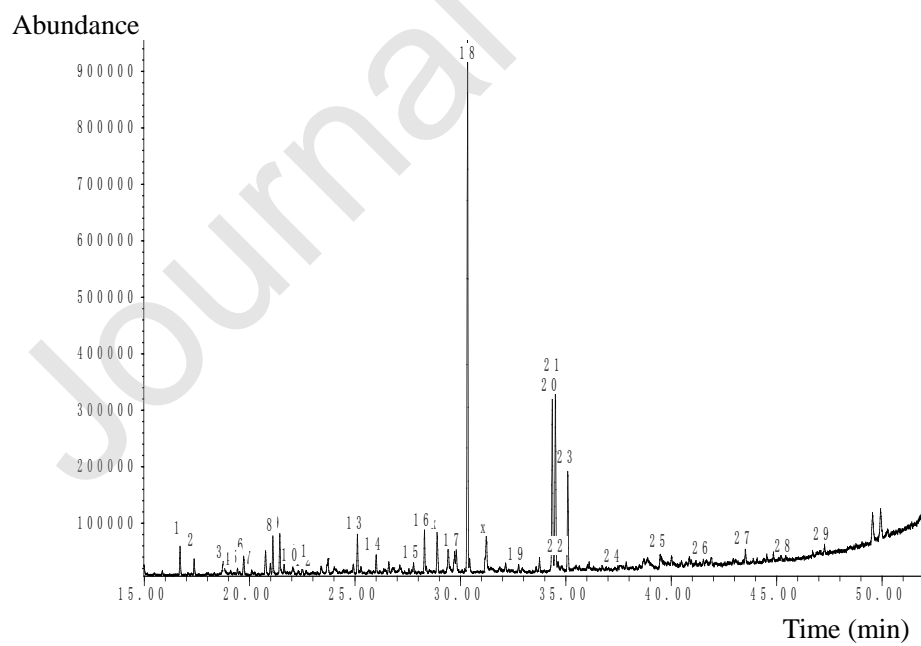


FIGURE 4. Total ion current chromatogram of polar fraction in treated sample from *H. verticillata*.

verticillata.

FIGURE 4

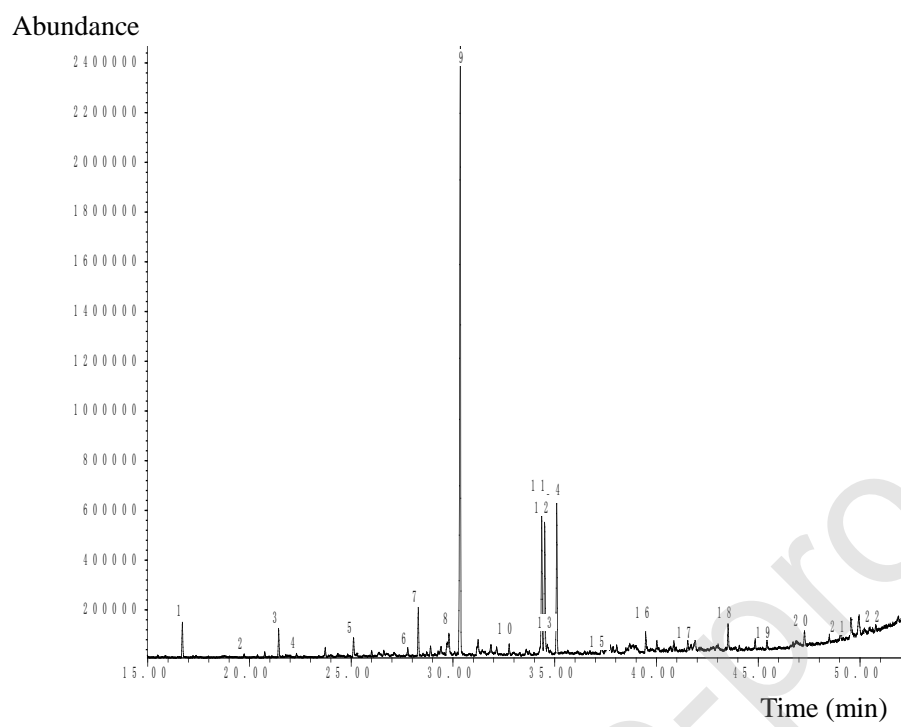


Table captions:

Table 1. Regression analysis between phenol concentration and time in the presence of *H. verticillata* system.

Table 1

| Initial phenol level (mg L ⁻¹) | Regression equation parameters | | | | |
|---|--------------------------------|-------------|--------------|--------|---------------|
| | C_0 | A | B | R^2 | $t_{1/2}$ (d) |
| 20 | 20.56 ± 0.40 | 6.41 ± 0.46 | 22.36 ± 1.73 | 0.9972 | 2.49 |
| 40 | 39.54 ± 0.88 | 6.39 ± 0.61 | 28.27 ± 2.89 | 0.9950 | 3.42 |
| 60 | 58.05 ± 1.06 | 7.55 ± 0.70 | 37.16 ± 3.63 | 0.9961 | 3.92 |
| 80 | 77.37 ± 1.40 | 8.65 ± 0.91 | 43.18 ± 4.76 | 0.9962 | 3.99 |
| 100 | 100.28 ± 2.15 | 6.82 ± 0.71 | 34.64 ± 3.80 | 0.9940 | 4.08 |
| 200 | 199.78 ± 2.28 | 0.04 ± 0.21 | 9.82 ± 1.53 | 0.9810 | 264.4 |

Footnote of Table 1:

Values are expressed as the mean ± SD ($P < 0.05$).

Table 2. Effects of phenol concentration on physiological parameters of *H. verticillata*.**Table 2**

| Initial phenol conc. (mg L ⁻¹) | physiological parameters | | | | | | | | | | | | | | |
|--|--------------------------------------|--------------------------------------|-----------------------------|-------------------------|----------------------------|-------------------------|--------------------------------|----------------------------|--------------------------------------|-------------------------|-------------------------|-------------------------------|--|--|--|
| | chl- <i>a</i> (mg FW ⁻¹) | chl- <i>b</i> (mg FW ⁻¹) | chls (mg FW ⁻¹) | Ratio of chl <i>a:b</i> | car (mg FW ⁻¹) | Ratio of chls:c | Protein (mg FW ⁻¹) | FAA (mg FW ⁻¹) | Soluble sugar (mg FW ⁻¹) | AsA (mg/100 g FW) | Δ FW (g) | MDA (nmol g ⁻¹ FW) | POD (U min ⁻¹ g ⁻¹ FW) | SOD (U min ⁻¹ g ⁻¹ FW) | O ₂ ^{-•} (nmol min ⁻¹ g ⁻¹ FW) |
| 0 | 0.90±0.11 ^a | 0.43±0.01 ^a | 1.33±0.11 ^a | 2.09±0.25 ^a | 0.16±0.01 ^a | 8.22±0.90 ^a | 8.32±0.44 ^a | 15.00±2.98 ^a | 1.42±0.14 ^c | 22.4±3.1 ^c | 2.33±1.57 ^a | 23.4±1.2 ^c | 1733.7±179.9 ^b | 0.92±0.03 ^f | 4.67±0.52 ^d |
| 20 | 0.87±0.19 ^a | 0.42±0.15 ^a | 1.33±0.30 ^a | 1.93±0.32 ^a | 0.16±0.06 ^a | 8.41±2.30 ^a | 7.30±0.71 ^{ab} | 12.16±2.03 ^{ab} | 2.69±0.56 ^b | 54.4±13.8 ^{bc} | 1.33±0.72 ^{ab} | 29.8±0.4 ^c | 1483.4±638.3 ^b | 1.43±0.06 ^e | 6.85±0.94 ^c |
| 40 | 0.80±0.11 ^{ab} | 0.35±0.05 ^a | 1.15±0.16 ^{ab} | 2.29±0.11 ^a | 0.16±0.03 ^a | 7.08±0.92 ^{ab} | 6.95±0.72 ^{ab} | 11.53±1.90 ^{ab} | 3.00±0.23 ^b | 59.7±6.8 ^{bc} | 0.63±0.21 ^{bc} | 38.6±1.6 ^b | 1688.7±285.6 ^b | 2.07±0.01 ^d | 8.70±0.60 ^b |
| 60 | 0.77±0.26 ^{ab} | 0.34±0.10 ^a | 1.10±0.36 ^{ab} | 2.27±0.30 ^a | 0.16±0.05 ^a | 6.87±0.65 ^{ab} | 6.07±1.26 ^{bc} | 11.94±4.26 ^{ab} | 2.88±0.44 ^b | 90.5±11.6 ^{ab} | 0.33±0.15 ^{bc} | 61.0±4.0 ^a | 1400.0±255.1 ^b | 2.17±0.04 ^c | 10.40±0.54 ^a |
| 80 | 0.78±0.14 ^{ab} | 0.37±0.11 ^a | 1.15±0.22 ^{ab} | 2.14±0.35 ^a | 0.16±0.02 ^a | 7.45±1.24 ^{ab} | 5.76±1.00 ^{bc} | 9.18±1.59 ^b | 3.00±0.27 ^b | 108.7±38.3 ^a | 0.30±0.36 ^{bc} | 45.7±1.5 ^b | 1348.8±354.3 ^b | 2.31±0.03 ^a | 8.24±0.31 ^b |
| 100 | 0.56±0.30 ^{ab} | 0.34±0.27 ^a | 1.00±0.46 ^{ab} | 2.09±0.54 ^a | 0.16±0.05 ^a | 7.29±2.30 ^{ab} | 5.01±1.29 ^c | 8.87±2.01 ^b | 3.11±0.66 ^{ab} | 127.3±12.1 ^a | 0.27±0.21 ^{bc} | 41.7±4.0 ^b | 1934.3±259.3 ^{ab} | 2.26±0.04 ^{ab} | 6.59±0.33 ^c |
| 200 | 0.47±0.07 ^b | 0.20±0.02 ^a | 0.67±0.08 ^b | 2.08±0.38 ^a | 0.15±0.04 ^a | 5.17±1.01 ^b | 4.80±0.88 ^c | 8.89±2.07 ^b | 3.81±0.39 ^a | 127.5±16.6 ^a | -0.06±0.11 ^c | 40.9±5.7 ^b | 2576.5±739.0 ^a | 2.23±0.02 ^b | 5.13±0.27 ^d |

Footnote of Table 2:

Values are expressed as the mean ± SD. Variants possessing the same letter are not statistically significant at

$P < 0.05$.

Table 3. Correlation between physiological parameters of *H. verticillata***Table 3**

| | Phenol conc. | chl- <i>a</i> | chl- <i>b</i> | car | Protein | FAA | Soluble sugar | AsA | MDA | POD | SOD | O ₂ ⁻ |
|-----------------------------|-----------------|---------------|---------------|--------------|----------------|----------------|------------------|---------------|-------------|--------|-------|-----------------------------|
| Phenol conc. | 1 | | | | | | | | | | | |
| chl- <i>a</i> | -0.941* * | 1 | | | | | | | | | | |
| chl- <i>b</i> | -0.951* * | 0.890** | 1 | | | | | | | | | |
| car | -0.857* * | 0.732 | 0.874* | 1 | | | | | | | | |
| Protein | -0.884* * | 0.899** | 0.796* | 0.524 | 1 | | | | | | | |
| FAA | -0.801* * | 0.797* | 0.674 | 0.427 | 0.938** | 1 | | | | | | |
| Soluble sugar | 0.831* * | -0.781* * | -0.825* * | -0.592 | -0.874* * | -0.885** ** | 1 | | | | | |
| AsA | 0.856* * | -0.868* * | -0.741 | -0.473 | -0.995** ** | -0.947** ** | 0.843* * | 1 | | | | |
| MDA | 0.364 | -0.327 | -0.421 | -0.027 | -0.613 | -0.463 | 0.541 | 0.607 | 1 | | | |
| POD | -0.767* * | -0.797* * | -0.782* * | -0.874* * | -0.469 | -0.371 | 0.453 | 0.413 | -0.181 | 1 | | |
| SOD | 0.674 | -0.661 | -0.659 | -0.264 | -0.883** ** | -0.879** ** | 0.866* * | 0.876** ** | 0.781* * | 0.157 | 1 | |
| O ₂ ⁻ | -0.198 | 0.229 | 0.085 | 0.455 | -0.122 | -0.107 | 0.229 | 0.122 | 0.780* * | -0.643 | 0.508 | 1 |

Footnote of Table 3:

*Correlation is significant at the 0.05 level (2-tailed).

**Correlation is significant at the 0.01 level (2-tailed).

Table 4. Non-polar fraction identification in control and treated samples of *H. verticillata*.**Table 4**

| Peak No. (P.N.) | Molecular Formula (M.F.) | Molecular Weight (M.W.) | Compounds | Content (%) | |
|--------------------|---------------------------------|----------------------------|----------------------------|-------------|---------|
| | | | | Control | Treated |
| 1 | C ₁₅ H ₃₂ | 212 | Pentadecane | 0.173 | 0.316 |
| 2 | C ₁₆ H ₃₄ | 226 | Hexadecane | 2.125 | 2.551 |
| 3 | C ₁₈ H ₃₈ | 254 | nor-pristane | 0.501 | 0.666 |
| 4 | C ₁₇ H ₃₆ | 240 | Heptadecane | 2.259 | 2.176 |
| 5 | C ₁₉ H ₄₀ | 268 | Pristane | 0.896 | 0.893 |
| 6 | C ₁₈ H ₃₈ | 254 | Octadecane | 2.532 | 2.461 |
| 7 | C ₂₀ H ₄₂ | 282 | Phytane | 1.035 | 1.006 |
| 8 | C ₁₉ H ₄₀ | 268 | Nonadecane | 2.838 | 3.423 |
| 9 | C ₂₀ H ₄₂ | 282 | Eicosane | 1.701 | 1.665 |
| 10 | C ₂₁ H ₄₄ | 296 | Heneicosane | 22.988 | 27.678 |
| 11 | C ₂₂ H ₄₆ | 310 | Docosane | 3.053 | 3.459 |
| 12 | C ₂₃ H ₄₈ | 324 | Tricosane | 31.858 | 30.305 |
| 13 | C ₂₄ H ₅₀ | 338 | Tetracosane | 3.393 | 4.490 |
| 14 | C ₂₅ H ₅₂ | 352 | Pentacosane | 11.403 | 10.499 |
| 15 | C ₂₆ H ₅₄ | 366 | Hexacosane | 3.849 | 2.132 |
| 16 | C ₂₅ H ₅₂ | 352 | Pentamethyl-eicosane (PMI) | 2.285 | 3.963 |
| 17 | C ₂₇ H ₅₆ | 380 | Heptacosane | 5.998 | 1.592 |
| 18 | C ₂₈ H ₅₈ | 394 | Octacosane | 0.435 | 0.382 |
| 19 | C ₂₉ H ₆₀ | 408 | Nonacosane | 0.677 | 0.342 |

Table 5. Analytical data of non-polar and polar fractions in the control and treated samples from *H. verticillata*.

Table 5

| Samples | non-polar fraction parameters | | | | | polar fraction parameters | | | |
|---------|---|---------------------------|-----------------|------|---------------------------------|---|---------------------------|--|-----------------|
| | Carbon number distribution | Main peak | $CPI_{total-1}$ | OEP | $\sum C_{21}^- / \sum C_{22}^+$ | Carbon number distribution of normal fatty acid | Main peak | \sum unsaturated fatty acids/ \sum saturated fatty acid | $CPI_{total-2}$ |
| Control | <i>n</i> -C ₁₅ — <i>n</i> -C ₂₉ | <i>n</i> -C ₂₃ | 4.58 | 8.75 | 0.57 | <i>n</i> -C ₁₂ — <i>n</i> -C ₂₄ | <i>n</i> -C ₁₆ | 0.515 | 0.684 |
| Treated | <i>n</i> -C ₁₅ — <i>n</i> -C ₂₉ | <i>n</i> -C ₂₃ | 4.45 | 6.92 | 0.76 | <i>n</i> -C ₁₄ — <i>n</i> -C ₂₆ | <i>n</i> -C ₁₆ | 0.348 | 0.640 |

Footnote of Table 5:

Note: $CPI_{total-1} = \sum \text{odd } C_n / \sum \text{even } C_n$; C_n , the relative content of *n*-alkanes when the length of the carbon chain was *n*. odd-even predominance (OEP) of *n*-alkanes, $OEP = C_{21} + 6C_{23} + C_{25} / 4(C_{22} + C_{24})$; $\sum C_{21}^-$, the total amount of *n*-alkanes before C_{21} ; $\sum C_{22}^+$, the total amount of *n*-alkanes after C_{22} . \sum unsaturated fatty acids and \sum saturated fatty acids represent the total amount of unsaturated and saturated normal fatty acids, respectively; $CPI_{total-2} = \sum \text{odd } C_n / \sum \text{even } C_n$, where C_n represents the relative content of normal fatty acids when the carbon chain length was *n*.

Table 6. Weak polarity fraction identification in *H. verticillata* (control and treated samples).**Table 6**

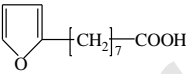
| Peak No. | M. F. | M. W. | Compounds | Content (%) | |
|----------|--|-------|---|-------------|---------|
| | | | | Control | Treated |
| 1 | C ₁₈ H ₃₄ O | 266 | norPristane-13-ene -2- ketone | 5.908 | 7.018 |
| 2 | C ₁₄ H ₁₀ | 178 | Phenanthrene | 4.013 | 4.146 |
| 3 | C ₂₀ H ₃₈ | 278 | Neophytadiene | 37.583 | 32.157 |
| 4 | C ₂₀ H ₃₈ | 278 | Neophytadiene | 7.472 | 4.914 |
| 5 | C ₂₀ H ₃₈ | 278 | Neophytadiene | 1.924 | 2.129 |
| 6 | C ₂₀ H ₃₈ | 278 | Neophytadiene | 13.780 | 9.060 |
| 7 | C ₁₅ H ₁₂ | 192 | Phenanthrene, 3-methyl- | 0.935 | 1.332 |
| 8 | C ₁₅ H ₁₂ | 192 | Phenanthrene, 2-methyl- | 2.661 | 3.319 |
| 9 | C ₁₅ H ₁₂ | 192 | Phenanthrene, 9-methyl- | 1.747 | 1.506 |
| 10 | C ₂₀ H ₃₆ O | 292 | 3-methyl-2-(3.7.11-trimethyldodecyl)furan | 7.762 | 9.564 |
| 11 | C ₁₅ H ₁₂ | 192 | Phenanthrene, 1-methyl- | 0.595 | 0.846 |
| 12 | | | Unknown | 5.052 | 6.036 |
| 13 | C ₂₀ H ₃₆ O | 292 | 3- (4.8.12-trimethyldodecyl) furan | 3.774 | 4.797 |
| 14 | C ₁₆ H ₁₀ | 202 | Fluoranthene | 2.557 | 5.556 |
| 15 | C ₁₆ H ₁₀ | 202 | Pyrene | 1.581 | 3.936 |
| 16 | C ₂₀ H ₃₄ O ₃ | 322 | 2-Furancarboxylic acid, pentadecyl ester | 2.656 | 3.684 |

Table 7. Polar fraction identification in control samples from *H. verticillata*.**Table 7**

| P.N. | M.F | M.W. | Compounds | Content (%) | M.F. in plants | Corresponding compounds in plants |
|------|--|------|--|-------------|--|-----------------------------------|
| 1 | C ₁₀ H ₁₈ O ₃ | 186 | Nonanoic acid, 9-oxo-, methyl ester | 1.827 | C ₉ H ₁₆ O ₃ | |
| 2 | C ₁₀ H ₁₀ O ₄ | 194 | Dimethyl phthalate | 1.000 | C ₈ H ₆ O ₄ | |
| 3 | C ₁₀ H ₁₀ O ₄ | 194 | 1,3-Benzenedicarboxylic acid, dimethyl ester | 0.965 | C ₈ H ₆ O ₄ | |
| 4 | C ₁₀ H ₁₀ O ₄ | 194 | 1,4-Benzenedicarboxylic acid, dimethyl ester | 0.286 | C ₈ H ₆ O ₄ | |
| 5 | C ₁₃ H ₂₆ O ₂ | 214 | Dodecanoic acid, methyl ester | 0.417 | C ₁₂ H ₂₄ O ₂ | |
| 6 | C ₁₁ H ₁₆ O ₂ | 180 | 2(4H)-Benzofuranone, tetrahydro-4,4,7-trimethyl- | 1.490 | C ₁₁ H ₁₆ O ₂ | |
| 7 | C ₁₁ H ₂₀ O ₄ | 216 | Nonandioic acid, dimethyl ester | 0.296 | C ₉ H ₁₆ O ₄ | |
| 8 | C ₁₃ H ₁₈ O | 190 | 2-Butanone, 1-(2,3,6-trimethylphenyl)-5-methyl- | 2.398 | C ₁₃ H ₁₈ O | |
| 9 | C ₁₂ H ₂₂ O ₄ | 230 | nonandioic acid, dimethyl ester | 2.673 | C ₁₀ H ₁₈ O ₄ | |
| 10 | C ₁₃ H ₁₆ O | 188 | 2-Butenone, 1-(2,3,6-trimethylphenyl)- | 0.634 | C ₁₃ H ₁₆ O | |
| 11 | C ₁₃ H ₁₀ O | 182 | Benzophenone | 0.692 | C ₁₃ H ₁₀ O | |
| 12 | C ₁₄ H ₂₈ O ₂ | 228 | Tridecanoic acid, methyl ester | 0.385 | C ₁₃ H ₂₆ O ₂ | |
| 13 | C ₁₅ H ₃₀ O ₂ | 242 | Tetradecanoic acid, methyl ester | 2.659 | C ₁₄ H ₂₈ O ₂ | |
| 14 | C ₁₄ H ₁₂ O | 196 | 3-methylbenzophenone | 1.277 | C ₁₄ H ₁₂ O | |

| | | | | | | |
|----|--|-----|--|--------|--|--|
| 15 | C ₁₆ H ₃₂ O ₂ | 256 | Pentadecanoic acid, methyl ester | 0.796 | C ₁₅ H ₃₀ O ₂ | $\text{H}_3\text{C}-\left[\text{CH}_2\right]_{13}-\overset{\text{O}}{\parallel}{\text{C}}-\text{OH}$ |
| 16 | C ₁₈ H ₃₆ O | 268 | nor-Pristane-2-one | 2.804 | C ₁₈ H ₃₆ O | $\text{H}_3\text{C}-\overset{\text{CH}_3}{\underset{ }{\text{CH}}}-\left[\text{CH}_2\right]_3-\overset{\text{CH}_3}{\underset{ }{\text{CH}}}-\left[\text{CH}_2\right]_3-\overset{\text{CH}_3}{\underset{ }{\text{CH}}}-\left[\text{CH}_2\right]_3-\overset{\text{O}}{\parallel}{\text{C}}-\text{CH}_3$ |
| 17 | C ₁₇ H ₃₂ O ₂ | 268 | 9- Hexadecenoic acid, methyl ester | 1.784 | C ₁₆ H ₃₀ O ₂ | $\text{H}_3\text{C}-\left[\text{CH}_2\right]_5-\text{CH}=\text{CH}-\left[\text{CH}_2\right]_7-\text{COOH}$ |
| 18 | C ₁₇ H ₃₄ O ₂ | 270 | Hexadecanoic acid, methyl ester | 37.34 | C ₁₆ H ₃₂ O ₂ | $\text{H}_3\text{C}-\left[\text{CH}_2\right]_{14}-\overset{\text{O}}{\parallel}{\text{C}}-\text{OH}$ |
| 19 | C ₁₈ H ₃₆ O ₂ | 284 | Heptadecanoic acid, methyl ester | 0.804 | C ₁₇ H ₃₄ O ₂ | $\text{H}_3\text{C}-\left[\text{CH}_2\right]_{15}-\overset{\text{O}}{\parallel}{\text{C}}-\text{OH}$ |
| 20 | C ₁₉ H ₃₄ O ₂ | 294 | Octadecadienoic acid, methyl ester | 12.635 | C ₁₈ H ₃₂ O ₂ | $\text{H}_3\text{C}-\left[\text{CH}_2\right]_3-\left[\text{CH}_2-\text{CH}=\text{CH}\right]_2-\left[\text{CH}_2\right]_7-\text{COOH}$ |
| 21 | C ₁₉ H ₃₂ O ₂ | 292 | Octadecatrienoic acid, methyl ester | 13.427 | C ₁₈ H ₃₀ O ₂ | $\text{H}_3\text{C}-\left[\text{CH}_2-\text{CH}=\text{CH}\right]_3-\left[\text{CH}_2\right]_7-\text{COOH}$ |
| 22 | C ₁₉ H ₃₆ O ₂ | 296 | 9-Octadecenoic acid, methyl ester | 0.582 | C ₁₈ H ₃₄ O ₂ | $\text{H}_3\text{C}-\left[\text{CH}_2\right]_7-\text{CH}=\text{CH}-\left[\text{CH}_2\right]_7-\text{COOH}$ |
| 23 | C ₁₉ H ₃₈ O ₂ | 298 | Octadecanoic acid, methyl ester | 7.386 | C ₁₈ H ₃₆ O ₂ | $\text{H}_3\text{C}-\left[\text{CH}_2\right]_{16}-\overset{\text{O}}{\parallel}{\text{C}}-\text{OH}$ |
| 24 | C ₂₀ H ₄₀ O ₂ | 312 | Nonadecanoic acid, methyl ester | 0.623 | C ₁₉ H ₃₈ O ₂ | $\text{H}_3\text{C}-\left[\text{CH}_2\right]_{17}-\overset{\text{O}}{\parallel}{\text{C}}-\text{OH}$ |
| 25 | C ₂₁ H ₄₂ O ₂ | 326 | Eicosanoic acid, methyl ester | 1.967 | C ₂₀ H ₄₀ O ₂ | $\text{H}_3\text{C}-\left[\text{CH}_2\right]_{18}-\overset{\text{O}}{\parallel}{\text{C}}-\text{OH}$ |
| 26 | C ₂₂ H ₄₄ O ₂ | 340 | Heneicosanoic acid, methyl ester | 0.458 | C ₂₁ H ₄₂ O ₂ | $\text{H}_3\text{C}-\left[\text{CH}_2\right]_{19}-\overset{\text{O}}{\parallel}{\text{C}}-\text{OH}$ |
| 27 | C ₂₃ H ₄₆ O ₂ | 354 | Docosanoic acid, methyl ester | 1.164 | C ₂₂ H ₄₄ O ₂ | $\text{H}_3\text{C}-\left[\text{CH}_2\right]_{20}-\overset{\text{O}}{\parallel}{\text{C}}-\text{OH}$ |
| 28 | C ₂₄ H ₄₈ O ₂ | 368 | Tricosanoic acid, methyl ester | 0.471 | C ₂₃ H ₄₆ O ₂ | $\text{H}_3\text{C}-\left[\text{CH}_2\right]_{21}-\overset{\text{O}}{\parallel}{\text{C}}-\text{OH}$ |
| 29 | C ₂₅ H ₅₀ O ₂ | 382 | Tetracosanoic acid, methyl ester | 0.760 | C ₂₄ H ₄₈ O ₂ | $\text{H}_3\text{C}-\left[\text{CH}_2\right]_{22}-\overset{\text{O}}{\parallel}{\text{C}}-\text{OH}$ |

Table 8. Polar fraction identification in treated sample from *H. verticillata*.**Table 8**

| P.N. | M.F. | M.W. | Compound | Content (%) | M.F. in plants | Corresponding compounds in plants |
|------|--|------|---|-------------|--|--|
| 1 | C ₁₀ H ₁₈ O ₃ | 186 | Nonanoic acid, 9-oxo-, methyl ester | 2.326 | C ₉ H ₁₆ O ₃ | — |
| 2 | C ₁₁ H ₂₀ O ₃ | 200 | Decanoic acid, 10-oxo-, methyl ester | 0.296 | C ₁₀ H ₁₈ O ₃ | $\text{HO}-\overset{\text{O}}{\parallel}{\text{C}}-(\text{CH}_2)_8-\overset{\text{O}}{\parallel}{\text{C}}-\text{H}$ |
| 3 | C ₁₁ H ₁₈ O ₃ | 198 | Methyl, 10-oxo-8-decenoate | 1.922 | C ₁₀ H ₁₆ O ₃ | $\text{HO}-\overset{\text{O}}{\parallel}{\text{C}}-(\text{CH}_2)_6-\text{CH}=\text{CH}-\overset{\text{O}}{\parallel}{\text{C}}-\text{H}$ |
| 4 | C ₁₃ H ₂₀ O ₃ | 224 | Methyl, 8- (2-furyl) octanoate | 0.258 | C ₁₂ H ₁₈ O ₃ |  |
| 5 | C ₁₅ H ₃₀ O ₂ | 242 | Tetradecanoic acid, methyl ester | 1.390 | C ₁₄ H ₂₈ O ₂ | — |
| 6 | C ₁₆ H ₃₂ O ₂ | 256 | Pentadecanoic acid, methyl ester | 0.579 | C ₁₅ H ₃₀ O ₂ | — |
| 7 | C ₁₈ H ₃₆ O | 268 | nor-Pristane-2-one | 3.178 | C ₁₈ H ₃₆ O | — |
| 8 | C ₁₇ H ₃₂ O ₂ | 268 | 9- Hexadecenoic acid, methyl ester | 1.626 | C ₁₆ H ₃₀ O ₂ | — |
| 9 | C ₁₇ H ₃₄ O ₂ | 270 | Hexadecanoic acid, methyl ester | 47.062 | C ₁₆ H ₃₂ O ₂ | — |
| 10 | C ₁₈ H ₃₆ O ₂ | 284 | Heptadecanoic acid, methyl ester | 0.883 | C ₁₇ H ₃₄ O ₂ | — |
| 11 | C ₁₉ H ₃₄ O ₂ | 294 | 9.12-Octadecadienoic acid, methyl ester | 10.444 | C ₁₈ H ₃₂ O ₂ | — |
| 12 | C ₁₉ H ₃₂ O ₂ | 292 | 9.12.15-Octadecatrienoic acid, methyl ester | 10.515 | C ₁₈ H ₃₀ O ₂ | — |
| 13 | C ₁₉ H ₃₆ O ₂ | 296 | 9-Octadecenoic acid, methyl ester | 1.181 | C ₁₈ H ₃₄ O ₂ | — |
| 14 | C ₁₉ H ₃₈ O ₂ | 298 | Octadecanoic acid, methyl ester | 10.684 | C ₁₈ H ₃₆ O ₂ | — |
| 15 | C ₂₀ H ₄₀ O ₂ | 312 | Nonadecanoic acid, methyl ester | 0.791 | C ₁₉ H ₃₈ O ₂ | — |
| 16 | C ₂₁ H ₄₂ O ₂ | 326 | Eicosanoic acid, methyl ester | 1.48 | C ₂₀ H ₄₀ O ₂ | — |
| 17 | C ₂₂ H ₄₄ O ₂ | 340 | Heneicosanoic acid, methyl ester | 0.788 | C ₂₁ H ₄₂ O ₂ | — |
| 18 | C ₂₃ H ₄₆ O ₂ | 354 | Docosanoic acid, methyl ester | 1.886 | C ₂₂ H ₄₄ O ₂ | — |
| 19 | C ₂₄ H ₄₈ O ₂ | 368 | Tricosanoic acid, methyl ester | 0.613 | C ₂₃ H ₄₆ O ₂ | — |
| 20 | C ₂₅ H ₅₀ O ₂ | 382 | Tetracosanoic acid, methyl ester | 1.181 | C ₂₄ H ₄₈ O ₂ | — |
| 21 | C ₂₆ H ₅₂ O ₂ | 396 | Pentacosanoic acid, methyl ester | 0.456 | C ₂₅ H ₅₀ O ₂ | $\text{H}_3\text{C}-(\text{CH}_2)_{23}-\overset{\text{O}}{\parallel}{\text{C}}-\text{OH}$ |
| 22 | C ₂₇ H ₅₄ O ₂ | 410 | Hexacosanoic acid, methyl ester | 0.463 | C ₂₆ H ₅₂ O ₂ | $\text{H}_3\text{C}-(\text{CH}_2)_{24}-\overset{\text{O}}{\parallel}{\text{C}}-\text{OH}$ |

Footnote of Table 8:

Note: —see Table 7.